

The N-Body Problem

November 2024

Felipe Sandoval
Georgia Institute of Technology
School of Earth and Atmospheric Science
fsandoval@gatech.edu

I. INTRODUCTION

During the 17th Century, mathematicians attempted to create models that could describe the motion of bodies under the influence of each other. The interaction of celestial bodies was of particular interest at the time. This study led to not only accurate equations to describe planetary motion, but also one of the first formulations of calculus [1]. Based on Johannes Kepler's study on elliptical orbits, Isaac Newton [2] described what in the present day would be referred to as a gravitational Two-Body Problem (2BP), where a central force enacts a force between two objects in correspondence with the inverse square law.

At the end of the 19th century, Henri Poincaré tackled an extension of Newton's study, that is, the motion of three bodies undergoing Newtonian mechanics, or the Three-Body Problem (3BP) [3]. The particular interest was that of the Earth-Moon-Sun system. Unlike the 2BP, the 3BP was found to have no general analytical solution, creating the basis for chaos theory. In the late 20th century, with the advent of modern computers, the 3BP was approached from a numerical standpoint, approximating and finding viable solutions for practical applications.

To completely generalize the problem, in the late 20th century, Levon Babadzanjanjanz conceptualized the N-Body Problem (NBP) [4], the interaction between an arbitrary number of celestial bodies. In the years between the 2BP and the NBP there may seem to be no other reason than scientific curiosity to work on solving these. However, since the success of the first spacecrafts in the 1950's, it has become a modern necessity to be able to find exact solutions or approximations in the area of orbital mechanics. Satellite orbit calculations require high-accuracy simulations to determine feasible mission parameters.

The objective of this paper is to develop an open-source framework to calculate the orbits of an arbitrary number of celestial bodies which can be easily implemented for specific applications. This is achieved through a custom-built numerical solver in Python. The accuracy of this simulating tool is assessed by its accuracy as compared to analytical solutions, and real data on the motion of the planets within the Solar System.

II. FORMULATION

To build up to the NBP model, the process is simplified starting with the 2BP and 3BP. These models rely on the assumption that the forces enacted follow the inverse square law presented by Newton in [2], and that the bodies act as if all the mass were contained at the center of them, or so called "point-masses."

2.1 Newtonian Mechanics and the 2BP

Consider the situation seen in Figure 2.1, where object A is found to be in the presence of another object, object B, of equal mass.

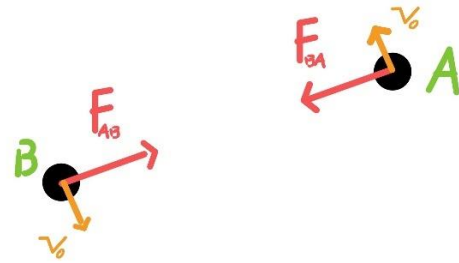


Figure 2.1: Two-Body System

Where object A has initial velocity " v_0 ". Thus, utilizing Newton's equation of motion:

$$\vec{F}_{BA} = m_A \vec{a}_{BA} \quad (2.1)$$

Where the acceleration of the orbiting body has the form:

$$\vec{a}_{BA} = -Gm_B \frac{\vec{r}_A - \vec{r}_B}{|\vec{r}_A - \vec{r}_B|^3} \quad (2.2)$$

Where:

\vec{F} is the force exerted

\vec{a} is the acceleration imparted

m_A & m_B are the masses of objects A and B respectively

\vec{r}_A & \vec{r}_B are the positions of objects A and B respectively

G is a conversion constant referred to as the "Gravitational Constant"

Equation (2.2) can then be rewritten as a differential equation such that the position of object A changes as:

$$\partial_t^2 \vec{r}_A = -Gm_B \frac{\vec{r}_A - \vec{r}_B}{|\vec{r}_A - \vec{r}_B|^3} \quad (2.3)$$

And in extension, the position of object B changes as:

$$\partial_t^2 \vec{r}_B = -Gm_A \frac{\vec{r}_B - \vec{r}_A}{|\vec{r}_B - \vec{r}_A|^3} \quad (2.4)$$

Where:

$\partial_t^2 \vec{r}$ is the second time derivative of position

2.2 Analytical solution for the 2BP

As hinted in section I, the 2BP can be solved analytically. To illustrate the accuracy of the numerical scheme, a case as the one seen in Figure 2.1 is used. The general solution as derived in [2] illustrates the fact and each body independently orbits the center of mass of the system

“ \vec{M}_{center} ”:

$$\vec{M}_{center}(t) = \frac{m_A \vec{r}_A(t) + m_B \vec{r}_B(t)}{m_A + m_B}$$

With this, the positions of the bodies are found to be:

$$\begin{aligned} \vec{r}_A(t) &= \vec{M}_{center}(t) + \frac{m_A}{m_A + m_B} \vec{r}_{AB} \\ \vec{r}_B(t) &= \vec{M}_{center}(t) + \frac{m_B}{m_A + m_B} \vec{r}_{BA} \end{aligned}$$

To simplify the comparison to the numerical solution, it will be assumed that $m_A = m_b = m$. Also, the initial positions and velocities of the bodies are set to be:

$$\begin{aligned} \vec{r}_{A0} &= -\vec{r}_{B0} = (1, 0, 0) \\ \vec{v}_{A0} &= -\vec{v}_{B0} = (0, v_0, 0) \end{aligned}$$

By doing this, the center of mass is calculated to be:

$$M_{center} = 2m$$

Located at the origin as seen in Figure 2.2

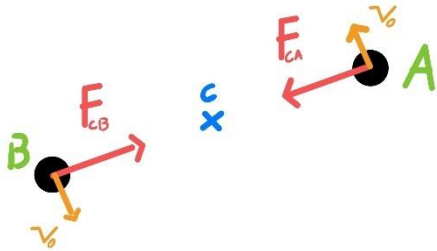


Figure 2.2: Two-Body System with Center of Mass C

With the assumption of equal masses, distances from the center of mass, and initial velocities, it can be derived that:

$$\partial_t M_{center} = 0$$

Meaning that the center of mass does not move from the origin, thus pointing to the fact that both bodies will

exhibit circular motion around the center of mass. This fact leads to simplifying the problem to a one body problem, where only the contributions from the center of mass are considered. This situation is represented in Figure 2.3.

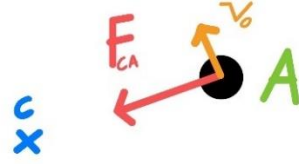


Figure 2.3: New One-Body System

The velocity v_0 can be calculated by assuming the bodies will experience circular motion, which acquire the centripetal acceleration:

$$\vec{a} = -\frac{v_0^2}{\vec{r}}$$

Thus, the acceleration on the bodies will be:

$$\vec{a} = -G \frac{2m}{|\vec{r}|^2} = -\frac{v_0^2}{|\vec{r}|}$$

Yielding the initial velocity:

$$v_0 = \sqrt{G \frac{2m}{|\vec{r}|}}$$

From this, the position of the bodies is found to be:

$$\begin{aligned} \vec{r}_A(t) &= |\vec{r}|(\cos(\theta), \sin(\theta), 0) \\ \vec{r}_B(t) &= -|\vec{r}|(\cos(\theta), \sin(\theta), 0) \end{aligned}$$

Or simplified:

$$\vec{r}_A = -\vec{r}_B = (\cos(\theta), \sin(\theta), 0) \quad (2.5)$$

With:

$$\theta = \frac{2\pi |\vec{r}|}{v_0} t$$

2.3 Numerical Solution for the 2BP

To give a basis to numerically solve the 3BP and NBP, the same scheme used for these is presented to solve the 2BP, and subsequently its accuracy is compared to that of the analytical solution seen in section 2.2.

Although the final model utilizes the 4th order Runge-Kutta scheme (RK4), the Euler-Forward (EF) scheme is presented here to give a better understanding of the process. The EF scheme can also be thought of as the 1st order Runge-Kutta scheme (RK1).

Starting with Equations (2.3-2.4):

$$\begin{aligned} \partial_t^2 \vec{r}_A &= -Gm_B \frac{\vec{r}_A - \vec{r}_B}{|\vec{r}_A - \vec{r}_B|^3} \\ \partial_t^2 \vec{r}_B &= -Gm_A \frac{\vec{r}_B - \vec{r}_A}{|\vec{r}_B - \vec{r}_A|^3} \end{aligned}$$

The differential equation can be rewritten in terms of the first time derivative of velocity, that is:

$$\begin{aligned}\partial_t^2 \vec{r}_A &= \partial_t \vec{v}_A \\ \partial_t^2 \vec{r}_B &= \partial_t \vec{v}_B\end{aligned}$$

Thus:

$$\begin{aligned}\partial_t \vec{v}_A &= -Gm_B \frac{\vec{r}_A - \vec{r}_B}{|\vec{r}_A - \vec{r}_B|^3} \\ \partial_t \vec{v}_B &= -Gm_A \frac{\vec{r}_B - \vec{r}_A}{|\vec{r}_B - \vec{r}_A|^3}\end{aligned}$$

By reducing the order of the differential equation, the problem can be solved as a system of 2 first order differential equations.

Taylor-expanding these derivatives, using the EF scheme, it can be found that:

$$\begin{aligned}\frac{\vec{v}_A(t + \Delta t) - \vec{v}_A(t)}{\Delta t} &= -Gm_B \frac{\vec{r}_A - \vec{r}_B}{|\vec{r}_A - \vec{r}_B|^3} \\ \frac{\vec{v}_B(t + \Delta t) - \vec{v}_B(t)}{\Delta t} &= -Gm_A \frac{\vec{r}_B - \vec{r}_A}{|\vec{r}_B - \vec{r}_A|^3}\end{aligned}$$

Isolating the velocities after a time step Δt :

$$\begin{aligned}\vec{v}_A(t + \Delta t) &= \vec{v}_A(t) - Gm_B \frac{\vec{r}_A - \vec{r}_B}{|\vec{r}_A - \vec{r}_B|^3} \Delta t \\ \vec{v}_B(t + \Delta t) &= \vec{v}_B(t) - Gm_A \frac{\vec{r}_B - \vec{r}_A}{|\vec{r}_B - \vec{r}_A|^3} \Delta t\end{aligned}$$

The same process can be used for the position, namely:

$$\begin{aligned}\frac{\vec{r}_A(t + \Delta t) - \vec{r}_A(t)}{\Delta t} &= \vec{v}_A \\ \frac{\vec{r}_B(t + \Delta t) - \vec{r}_B(t)}{\Delta t} &= \vec{v}_B\end{aligned}$$

And isolating the positions after a time step Δt :

$$\begin{aligned}\vec{r}_A(t + \Delta t) &= \vec{r}_A(t) + \vec{v}_A(t) \Delta t \\ \vec{r}_B(t + \Delta t) &= \vec{r}_B(t) + \vec{v}_B(t) \Delta t\end{aligned}$$

So, the whole system can be described by:

$$\begin{aligned}\vec{v}_A(t + \Delta t) &= \vec{v}_A(t) - Gm_B \frac{\vec{r}_A - \vec{r}_B}{|\vec{r}_A - \vec{r}_B|^3} \Delta t \\ \vec{v}_B(t + \Delta t) &= \vec{v}_B(t) - Gm_A \frac{\vec{r}_B - \vec{r}_A}{|\vec{r}_B - \vec{r}_A|^3} \Delta t \\ \vec{r}_A(t + \Delta t) &= \vec{r}_A(t) + \vec{v}_A(t) \Delta t \\ \vec{r}_B(t + \Delta t) &= \vec{r}_B(t) + \vec{v}_B(t) \Delta t\end{aligned}$$

These solutions can then be put in a form more familiar for Runge-Kutta schemes, namely:

$$\begin{aligned}K_{1r} &= f_1(t_n, \vec{r}_n, \vec{v}_n) = \vec{v}_n \\ K_{1v} &= f_2(t_n, \vec{r}_n, \vec{v}_n) = -G \frac{M}{|\vec{r}|^3} \vec{r}\end{aligned}$$

With:

$$\begin{aligned}\vec{r}(t + \Delta t) &= K_{1r} \Delta t \\ \vec{v}(t + \Delta t) &= K_{1v} \Delta t\end{aligned}$$

Where:

K_{1r} denotes the position "K" value of the scheme
 K_{1v} denotes the velocity "K" value of the scheme
 \vec{v}_n denotes the velocity
 \vec{r}_n denotes the position
 Δt is the time step used

This derivation constitutes the first "K" value of RK4 as seen in [5]. Starting by defining:

$$f_1(t_n, \vec{r}_n, \vec{v}_n) = \vec{v}_n$$

And

$$f_2(t_n, \vec{r}_n, \vec{v}_n) = -G \frac{M}{|\vec{r}|^3} \vec{r}$$

All the "K" values can then be found to be:

$$\begin{aligned}K_{1r} &= f_1(t_n, \vec{r}_n, \vec{v}_n) \\ K_{2r} &= f_1\left(t_n + \frac{\Delta t}{2}, \vec{r}_n + K_{1r} \frac{\Delta t}{2}, \vec{v}_n + K_{1v} \frac{\Delta t}{2}\right) \\ K_{3r} &= f_1\left(t_n + \frac{\Delta t}{2}, \vec{r}_n + K_{2r} \frac{\Delta t}{2}, \vec{v}_n + K_{2v} \frac{\Delta t}{2}\right) \\ K_{4r} &= f_1(t_n + \Delta t, \vec{r}_n + K_{3r} \Delta t, \vec{v}_n + K_{3v} \Delta t) \\ \text{And} \\ K_{1v} &= f_2(t_n, \vec{r}_n, \vec{v}_n) \\ K_{2v} &= f_2\left(t_n + \frac{\Delta t}{2}, \vec{r}_n + K_{1r} \frac{\Delta t}{2}, \vec{v}_n + K_{1v} \frac{\Delta t}{2}\right) \\ K_{3v} &= f_2\left(t_n + \frac{\Delta t}{2}, \vec{r}_n + K_{2r} \frac{\Delta t}{2}, \vec{v}_n + K_{2v} \frac{\Delta t}{2}\right) \\ K_{4v} &= f_2(t_n + \Delta t, \vec{r}_n + K_{3r} \Delta t, \vec{v}_n + K_{3v} \Delta t)\end{aligned}$$

With:

$$\vec{r}(t + \Delta t) = \vec{r}(t) + \frac{\Delta t}{6} (K_{1r} + 2K_{2r} + 2K_{3r} + K_{4r}) \quad (2.6)$$

$$\vec{v}(t + \Delta t) = \vec{v}(t) + \frac{\Delta t}{6} (K_{1v} + 2K_{2v} + 2K_{3v} + K_{4v}) \quad (2.7)$$

The accuracy of this scheme is explored in part IV by comparing it with the analytical solution found in 2.2.

2.4 Extension to the 3BP and the NBP

A fact that comes from Newton's equation of motion is the superposition of forces, that is to say, the force imparted on a system with multiple bodies is equal to the sum of all forces individually. In the case with three bodies with positions \vec{r}_1 , \vec{r}_2 , and \vec{r}_3 , the force acting on body 1 is:

$$\vec{F}_1 = \vec{F}_{21} + \vec{F}_{31}$$

Or as written in a form as seen in Equation (2.3), the acceleration imparted on each body is:

$$\begin{aligned}\vec{a}_1 &= \partial_t^2 \vec{r}_1 = -Gm_2 \frac{\vec{r}_1 - \vec{r}_2}{|\vec{r}_1 - \vec{r}_2|^3} - Gm_3 \frac{\vec{r}_1 - \vec{r}_3}{|\vec{r}_1 - \vec{r}_3|^3} \\ \vec{a}_2 &= \partial_t^2 \vec{r}_2 = -Gm_1 \frac{\vec{r}_2 - \vec{r}_1}{|\vec{r}_2 - \vec{r}_1|^3} - Gm_3 \frac{\vec{r}_2 - \vec{r}_3}{|\vec{r}_2 - \vec{r}_3|^3} \\ \vec{a}_3 &= \partial_t^2 \vec{r}_3 = -Gm_1 \frac{\vec{r}_3 - \vec{r}_1}{|\vec{r}_3 - \vec{r}_1|^3} - Gm_2 \frac{\vec{r}_3 - \vec{r}_2}{|\vec{r}_3 - \vec{r}_2|^3}\end{aligned}$$

Or written in summation form:

$$\partial_t^2 \vec{r}_n = \sum_{i=1}^3 -Gm_i \frac{\vec{r}_n - \vec{r}_i}{|\vec{r}_n - \vec{r}_i|^3}, i \neq n$$

This equation can be generalized then to the case with N bodies:

$$\partial_t^2 \vec{r}_n = \sum_{i=1}^N -Gm_i \frac{\vec{r}_n - \vec{r}_i}{|\vec{r}_n - \vec{r}_i|^3}, i \neq n \quad (2.9)$$

$$n = 1, 2, \dots, N$$

And so, using the same scheme presented in section 2.3, the positions and velocities of each body can be calculated using RK4:

$$\vec{r}_n(t + \Delta t) = \vec{r}_n(t) + \frac{\Delta t}{6} (K_{1r} + 2K_{2r} + 2K_{3r} + K_{4r})$$

$$\vec{v}_n(t + \Delta t) = \vec{v}_n(t) + \frac{\Delta t}{6} (K_{1v} + 2K_{2v} + 2K_{3v} + K_{4v})$$

With:

$$f_1(t_n, \vec{r}_n, \vec{v}_n) = \vec{v}_n$$

$$f_2(t_n, \vec{r}_n, \vec{v}_n) = \sum_{i=1}^N -Gm_i \frac{\vec{r}_n - \vec{r}_i}{|\vec{r}_n - \vec{r}_i|^3}, i \neq n$$

(The implementation used for this paper can be seen in attachment “main.py” under the function RK4_step inside the CelestialBody class).

2.5 Choice of Time Step

An essential aspect of any numerical simulation is choosing a suitable time step based on certain parameters. As there is no general solution to the NBP as discussed in Section 1, there is a motivation to create a way to estimate this choice.

Looking at the parameters for the simulation, namely the initial position and velocity of the bodies, yields a satisfactory estimation.

Given the position $r(t)$ and velocity $v(t)$ of a body (Body A), the position of Body A after one time step Δt is:

$$r(t + \Delta t) = v(t)\Delta t$$

If the separation to the closest other body (Body B) is R , a sensible condition may be that the distance traveled by the body over a time step is smaller than half the separation:

$$r(t + \Delta t) = v(t)\Delta t < \frac{R}{2}$$

By assuming a circular orbit, the velocity can be substituted with a process identical to the one done in section 2.2, that is:

$$v = \sqrt{G \frac{M}{R}}$$

Leads to the condition:

$$v(t)\Delta t = \sqrt{G \frac{M}{R}} \Delta t < \frac{R}{2}$$

Or simplified:

$$\Delta t \leq \sqrt{\frac{R^3}{4GM}}$$

III. MODEL RESULTS

To examine the effectiveness of the RK4 scheme for this application, three examples are explored in this section, namely the 2BP scenario specified in 2.2, a simulation of the solar system, and an NBP following the initial conditions specified in [6].

3.1 2BP Example

With the initial conditions and simulation parameters from 2.2 as seen in Table 3.1:

Table 3.1: Simulation Parameters

Parameter	Value
Initial Position for Body A	(1,0,0) Au
Initial Position for Body B	(-1,0,0) Au
Initial Velocity for Body A	(0,3.141593,0) Au/yr
Initial Velocity for Body B	(0,-3.141593,0) Au/yr
Time Step	0.01 yr
Simulation Time	25 yr

The resulting orbit is as seen in Figure 3.1 and the plot for the “x” (horizontal) component of the bodies is as seen in Figure 3.2.

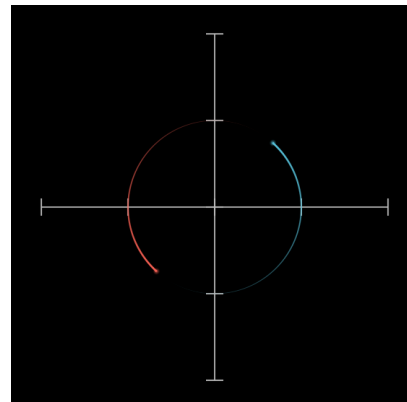


Figure 3.1: Resulting Orbits for the 2BP Case

A circular path around the origin is observed which agrees with the expectation set forth in Section 2.2. (See attachment “TwoBP.mp4” for the simulation video)

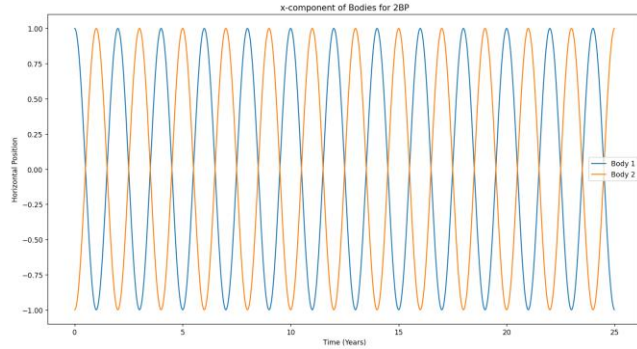


Figure 3.2: Plot of Position for 2BP

Very clear sinusoidal behavior is observed for the 2BP as made evident by the plot.

3.2 Solar System Example

To demonstrate the effectiveness at an astronomical scale, a simulation of the solar system was created, with the simulation parameters as seen in Table 3.2, and initial conditions as seen in Appendix A. The resulting orbits are as seen in Figure 3.3 and the plot of the “inner” solar system’s (Mercury, Venus, Earth, and Mars) horizontal component of position is as seen in Figure 3.4.

Table 3.2: Simulation Parameters

Parameter	Value
Time Step	0.01 yr
Simulation Time	50 yr

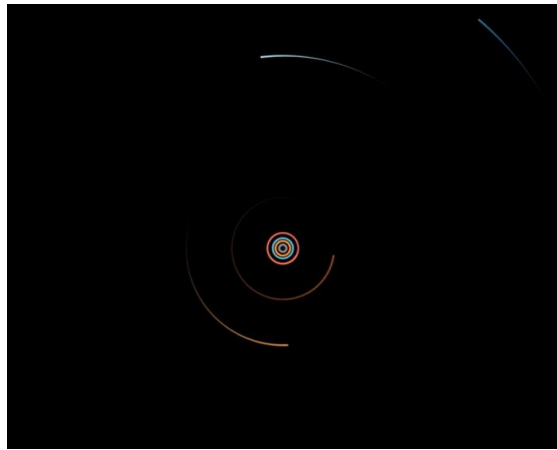


Figure 3.3: Resulting Orbits for Solar System Simulation

As seen in the figure, all the orbits appear circular in nature. See attachment “SolarSystem.mp4” for the simulation video)

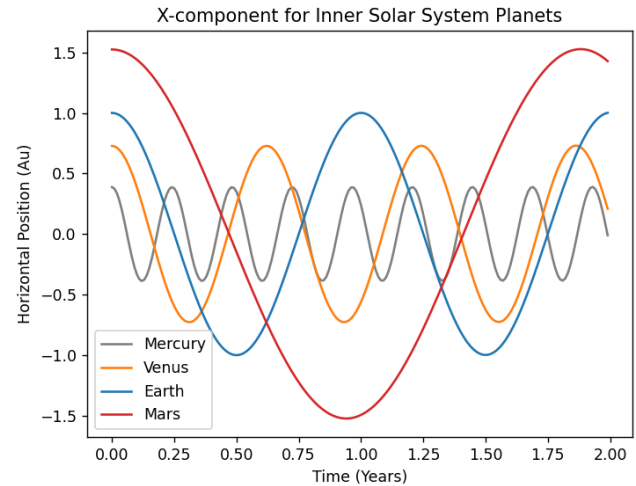


Figure 3.4: Resulting Orbits for Earth and Mars in Solar System Simulation

These orbital periods and the remaining ones are explored in Section 4.1.

3.3 Example with Large N

To showcase the versatility of this simulating tool, a non-practical example was devised. A common simulation with a periodic nature for the 3BP is the so called “Figure 8” [5].

An example of this is as seen in Figure 3.3 with the initial velocities as specified in [6] $v_x = 0.3471128135672417$ and $v_y = 0.5327268517676$. The initial conditions can be seen in Table 3.3.

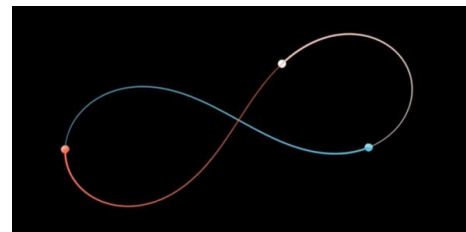


Figure 3.3: Figure 8 Orbit

(See attachment “Figure8.mp4” for simulation video)

Initial Position for Body 1	(1,0,0)
Initial Position for Body 2	(-1,0,0)
Initial Position for Body 3	(0,0,0)
Initial Velocity for Body 1	($v_x, v_y, 0$)
Initial Velocity for Body 2	($v_x, v_y, 0$)
Initial Velocity for Body 3	($-2v_x, -2v_y, 0$)
Time Step	0.01
Simulation Time	25

To demonstrate the power of the tool, a scene with four of these “Figure 8” orbits were placed orbiting a central “Figure 8,” as seen below in Figure 3.4.

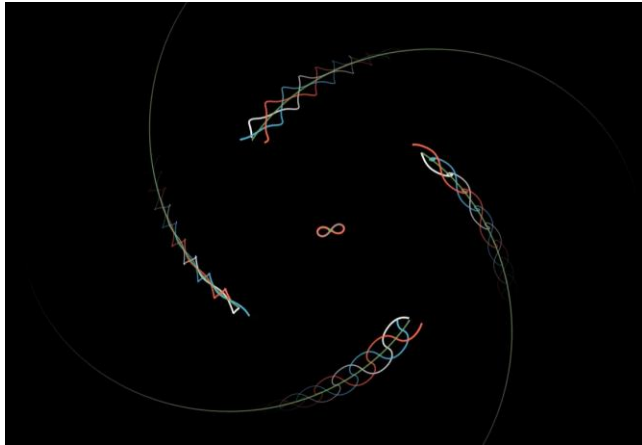


Figure 3.4: Figure 8 Orbits

(See attachment “OrbitingFigure8.mp4” for simulation video)

The simulation successfully calculates the complex orbits for these 12 bodies without problem.

IV. MODEL DISCUSSION

4.1 Analysis for Solar System Simulation

To verify the accuracy of the model used, an apparent parameter to explore would be the orbital period of a body around another. Using NASA’s data on orbital periods for the Solar System’s planets [7], the simulated periods are compared.

To do so, a Fast Fourier Transform (FFT) of the positions of the planets (Such as the one seen in Figure 3.4) is taken, yielding the frequency of oscillation f , which is translated into the orbital period T :

$$T = \frac{1}{f}$$

The results are as seen in Table 4.1

Table 4.1: Orbital Periods

Planet	Simulated Period (Earth Years)	Actual Period (Earth Years)	%Error
Mercury	0.238	0.241	1.24
Venus	0.6211	0.615	0.99
Earth	1.002	1.000	0.2
Mars	1.880	1.881	0.05
Jupiter	11.364	11.862	4.19
Saturn	29.412	29.447	0.12
Uranus	83.333	84.011	0.81
Neptune	166.667	164.79	1.14

The simulation was run for 500 years to account for the length of Neptune’s orbit as a larger sample was required. The same time step used in Section 3.2 was used, specifically $\Delta t = 0.01$ Years.

Evidently, this model yields precise results for the orbital periods. The slightly higher error of Mercury’s orbit may be due to the sampling frequency of the FFT not being small enough.

4.2 Model for Numerical Error Regarding Orbit Decay

To better understand the accuracy of the model for the general case, the numerical solution for the 2BP is compared against its analytical solution as found in Sections 3.1 and 2.2. With it, the error on the radius of the orbit is calculated.

With the assumptions made in Section 3.1, namely that the bodies are separated by 1 Au from the center of mass, the error is as seen in Figure 4.1. The parameters for the best fit line are as seen in Table 4.2.

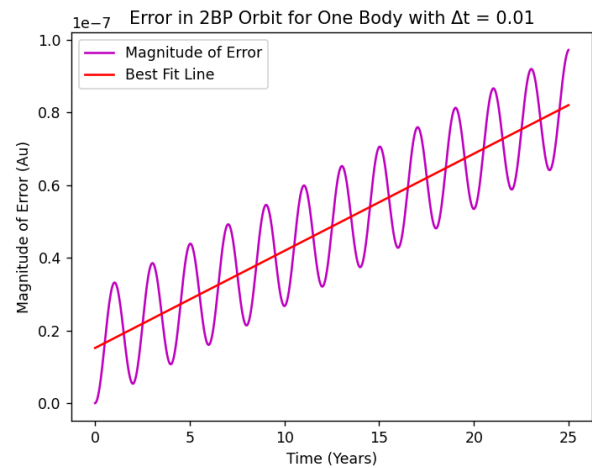


Figure 4.1: Error for 2BP

The error is calculated by finding the magnitude of the distance from the origin to the body. As the expected orbit is circular (constant radius), this value can then be subtracted from the expected value to find the error.

To find a suitable best fit line, a first order polynomial regression was used. This is to assure that the “average” error is used to disregard the oscillations. In this manner, the error is estimated to have a linear relationship over time.

Table 4.2: Best Fit Line Parameters

Parameter	Value
Slope	$2.67 * 10^{-9} \frac{\text{Au}}{\text{Year}}$
Vertical Offset	$1.52 * 10^{-8} \text{ Au}$

It is apparent from the plot that the error at this scale is negligible. Based on the Values from Table 3.1, specifically with time step:

$$\Delta t = 0.01 \text{ Years} \approx 4 \text{ Days}$$

Based on the parameters found on Table 4.1, the estimated error is:

$$\text{Error} \approx 2.67 \cdot 10^{-9} \frac{\text{Au}}{\text{Year}} = 400 \frac{\text{m}}{\text{Year}} = 1.1 \frac{\text{m}}{\text{Day}}$$

The same process can be repeated for varying magnitudes of Δt , as is done in Table 4.2, and the resulting plots are as seen in Figures 4.2-4.4.

Table 4.2: Error Slopes for Varying Time Steps

Time Step	Best Fit Error
0.05	$8.3 \cdot 10^{-6}$
0.01	$2.67 \cdot 10^{-9}$
0.005	$8.36 \cdot 10^{-11}$
0.001	$2.66 \cdot 10^{-14}$

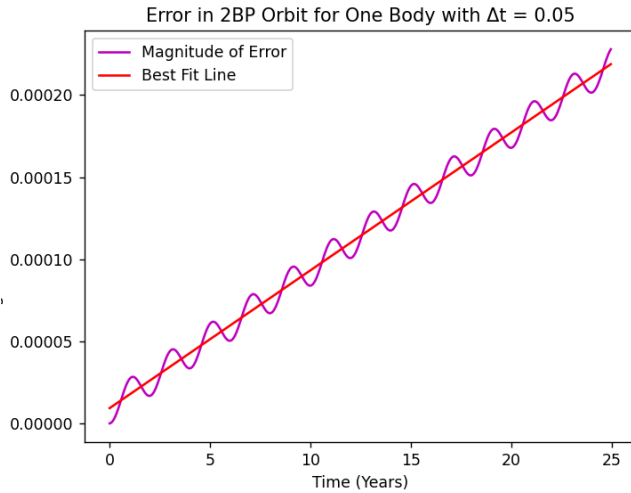


Figure 4.2: Error for 2BP with $\Delta t = 0.05$

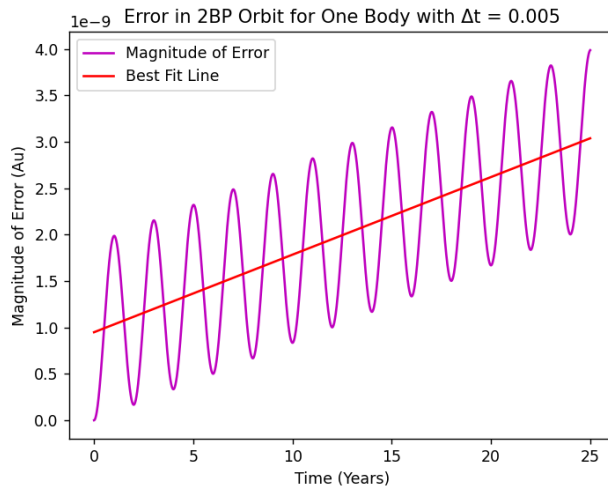


Figure 4.3: Error for 2BP with $\Delta t = 0.005$

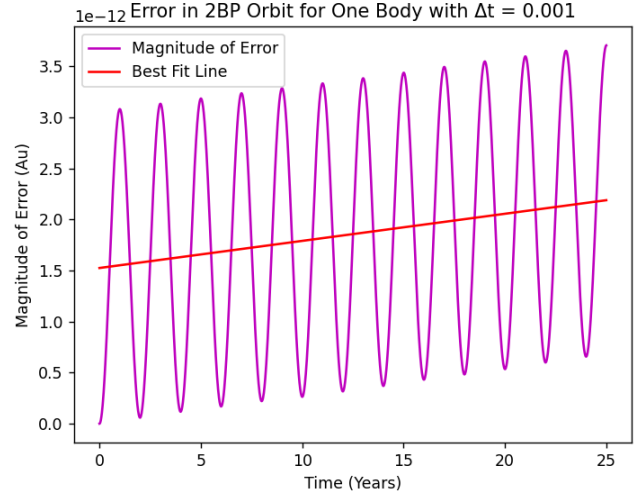


Figure 4.4: Error for 2BP with $\Delta t = 0.001$

Based on these calculations, an estimation of the order of magnitude of error over time can be made based on the time step used for the simulation.

$$O(\text{Error}) \approx O((\Delta t)^5 \cdot 10) \quad (4.1)$$

Note that Equation 4.1 is meant to be used as a practical way to estimate the error and is based on observation only.

Based on Equation 4.1, the validity of the simulation seen in Section 3.2 can be assessed. With the parameters from Table 3.2, the order of the error for Earth's orbit is expected to be:

$$(\Delta t)^5 \cdot 10 = (0.01)^5 \cdot 10 \approx 10^{-9} \frac{\text{Au}}{\text{Year}}$$

Which, over the simulation time of 50 years yields an expected error of:

$$50 \text{ Year} \cdot 10^{-9} \frac{\text{Au}}{\text{Year}} = 5 \cdot 10^{-8} \text{ Au} \approx 7.5 \text{ km}$$

With these results, the strength of this simulating tool is apparent.

V. SUMMARY

This report attempted to showcase the basis by which one may judge the accuracy of a numerical model for the NBP. The 4th order Runge-Kutta algorithm proved versatile and was adequate for this application. The numerical result illustrated that this tool may be used to estimate orbital periods or similar operations very accurately.

VI REFERENCES

- [1] Speiser, D., “*The Kepler Problem from Newton to Johann Bernoulli.*” Arch. Hist. Exact Sci. 50, 103–116. (1996).
- [2] Newton, I., “*Philosophiae Naturalis Principia Mathematica.*” Londini, Jussu Societatis Regiæ ac Typis Josephi Streater. Prostat apud plures Bibliopolas. (1687).
- [3] Wolfram, S., “*A new kind of science.*” Wolfram Media, 972. (2002).
- [4] Babadzanjan, L. K., “*Existence of the continuations in the N-body problem*”, Celestial Mechanics. (1979).
- [5] Cheever, E., “*Fourth Order Runge-Kutta.*” Swarthmore College. (2005-2022).
<<https://lpsa.swarthmore.edu/NumInt/NumIntFourth.html>>
- [6] Ramos, F. P., “*Stable Closed Orbits – Figure-8 Numerical study using MATLAB.*” University of Edinburgh, United Kingdom. (2019).
- [7] Williams, D. R., “*Planetary Fact Sheet – Metric.*” NASA Goddard Space Flight Center.
<<https://nssdc.gsfc.nasa.gov/planetary/factsheet/>>

VII APPENDIX

Appendix A

Initial conditions for Solar System Simulation

Body	Position (Au)	Velocity (Au/yr)	Mass (Solar Masses)
Sun	(0, 0, 0)	(0, 0, 0)	1
Mercury	(0.39, 0, 0)	(0, 10.09, 0)	$1.65 \cdot 10^{-7}$
Venus	(0.73, 0, 0)	(0, 7.36, 0)	$2.45 \cdot 10^{-6}$
Earth	(1, 0, 0)	(0, 6.28, 0)	$3 \cdot 10^{-6}$
Mars	(1.52, 0, 0)	(0, 5.09, 0)	$3.21 \cdot 10^{-7}$
Jupiter	(5.06, 0, 0)	(0, 2.79, 0)	$9.543 \cdot 10^{-4}$
Saturn	(9.64, 0, 0)	(0, 2.02, 0)	$2.857 \cdot 10^{-4}$
Uranus	(19.19, 0, 0)	(0, 1.43, 0)	$4.365 \cdot 10^{-5}$
Neptune	(29.89, 0, 0)	(0, 1.15, 0)	$5.149 \cdot 10^{-5}$

Appendix B

The visualization for this paper was done with Manim, a rendering tool developed to visualize mathematical operations. The simulation tool does not require this rendering library, but can be installed following directions at <https://github.com/3b1b/manim?tab=readme-ov-file#installation>.

Look at the function “example()” in the file main.py for a step-by-step example on how to plot the Figure 8.